Structural Engineering and Mechanics, Vol. 13, No. 5 (2002) 569-589
DOI: http://dx.doi.org/10.12989/sem.2002.13.5.569

Integrated equations of motion for direct integration methods

Shuenn-Yih Chang†

National Center for Research on Earthquake Engineering,
National Taiwan University, Taipei, Taiwan, R.O.C.

(Received April 7, 2000, Revised July 10, 2001, Accepted March 6, 2002)

Abstract. In performing the dynamic analysis, the step size used in a step-by-step integration method might be much smaller than that required by the accuracy consideration in order to capture the rapid changes of dynamic loading or to eliminate the linearization errors. It was first found by Chen and Robinson that these difficulties might be overcome by integrating the equations of motion with respect to time once. A further study of this technique is conducted herein. This include the theoretical evaluation and comparison of the capability to capture the rapid changes of dynamic loading if using the constant average acceleration method and its integral form and the exploration of the superiority of the time integration to reduce the linearization error. In addition, its advantage in the solution of the impact problems or the wave propagation problems is also numerically demonstrated. It seems that this time integration technique can be applicable to all the currently available direct integration methods.

Key words: time integration; smoothing effect; linearization errors.

1. Introduction

The direct integration method (Bathe and Wilson 1973, Hilber *et al*. 1977, Houbolt 1950, Newmark 1959, Park 1975, Zienkiewicz 1977) is the most widely used technique for nonlinear dynamic analysis and its computational effort is closely related to the size of time step. This is because that the use of a smaller time step will involve more computation steps for a given duration. However, the size of time step cannot be chosen arbitrarily. In fact, the size of time step for direct integration methods is constrained by:

(1) the presence of high-frequency modes,
(2) the rapid changes of dynamic loading,
(3) the abrupt changes in stiffness due to yielding or unloading, and
(4) the smooth variation of restoring force due to material and/or geometric nonlinearities.

Therefore, how to treat these difficulties is very important in practical applications. The causes of the difficulties and the available techniques to deal with the constraints can be found in Reference (Chang 1994 & 1996, Chang *et al*. 1998, Chang 1996, Chen and Robinson 1993). It is very

† Associate Research Fellow

promising to convert the second-order differential equations of motion into the first-order equations by integrating it with respect to time once as the new governing equations of motion in performing the direct integration. In fact, the conversion of equations of motion may automatically overcome the constraint (2), (3) and (4) and will be further investigated herein. This time integration technique originated from the development of the successive symmetrical quadratures method by Chen and Robinson (1993).

In earthquake engineering, the external force is generally expressed in terms of ground acceleration, which is usually a very rapidly changing function of time. It would then be assumed that the size of integration time step must be chosen so small that the rapid changes of dynamic loading can be captured. For a low-frequency input, there might be no limitation on the size of integration time step to trace the rapid changes of external excitation accurately. However, for a high-frequency input, a time step that is much smaller than that required by accuracy consideration, might be needed. Time integration of the equations of motion leads to the integration of external forces. Thus, the jagged character of the applied loading is removed from the integration process. If the external force is expressed in terms of ground acceleration, the time integral of this external force will be in terms of the ground velocity that is much smoother than the ground acceleration. The trapezoidal rule can be used to compute the time integral of external force for earthquake inputs before the step-by-step integration is performed.

In the direct integration methods, the whole process is approximated by a series of successively changing linear systems. In this procedure, the response is computed for a series of short time steps. Dynamic equilibrium is imposed at the start and the end of each time step. That is, the structural properties corresponding to the current deformed system is computed at the beginning of each time step in order to approximate the nonlinear behavior. Therefore, larger errors might be introduced if an abrupt change of material properties during the time step is not exactly captured or the smooth variation of the restoring force is not realistically reflected due to the presence of material and/or geometrical nonlinearities (Chang 1994, Chang *et al*. 1998, Chen and Robinson 1993). Abrupt changes of material properties may occur when the structural elements yield or are unloaded.

Abrupt changes in stiffness may result in significant errors in nonlinear dynamic analysis when a large time step is used. In addition, the smooth variation of the restoring force for nonlinear systems might lead to inaccurate solutions or even instability for a large time step even though the integration schemes are unconditionally stable for linear systems. Thus, it is very important to reduce the errors introduced by the assumption that the structural properties remain constant during each time step. Time integral of the restoring force is employed to replace the restoring force as the equations of motion are integrated with time. This indicates that the integral of restoring force is responsible for the approximation of the nonlinear behavior of the system. Obviously, it can provide more realistic simulation of the nonlinear behavior than the use of restoring force since the time history of resistance within each time step is entirely taken into account.

The detailed application of the time integration technique to the Newmark method is presented. The superiority of the time integration for the step-by-step integration procedure will be further studied numerically and/or theoretically. At first, the capability to capture the rapid changes of dynamic loading for the use of the constant average acceleration method and its integral form is theoretically evaluated and thoroughly compared. Meanwhile, the linearization errors occurred in a nonlinear system will be schematically sketched and compared for the original and integral forms. In addition, some numerical examples are used to demonstrate the advantages of the time integration of equations of motion.

2. Integral form of Newmark method

In the dynamic analysis, a structural system can be idealized as a discrete model. The equations of motion for the discrete structural model are generally expressed by a set of second-order ordinary differential equations and can be written in a matrix form as:

$$\boldsymbol{M}\ddot{\boldsymbol{u}} + \boldsymbol{C}\dot{\boldsymbol{u}} + \boldsymbol{K}\boldsymbol{u} = \boldsymbol{f} \tag{1}$$

where $\boldsymbol{M}$, $\boldsymbol{C}$ and $\boldsymbol{K}$ are the mass, viscous damping and stiffness matrices, $\boldsymbol{u}$, $\dot{\boldsymbol{u}}$ and $\ddot{\boldsymbol{u}}$ are the vectors of displacement, velocity and acceleration, respectively, and $\boldsymbol{f}$ is the applied force vector.

For simplicity, only a linear single-degree-of-freedom system is used to illustrate the application of the time integration technique to the Newmark method. The equation of motion for a single-degree-of-freedom system can be written as:

$$m\ddot{u} + c\dot{u} + ku = f \tag{2}$$

where m, c, and k are the mass, viscous damping and stiffness, u, $\dot{u}$ and $\ddot{u}$ are the displacement, velocity and acceleration, and f is the external force. For a nonlinear system, it is more appropriate to use the restoring force r to replace ku since the stiffness is no longer a constant in the nonlinear range. The initial value problem for Eq. (2) is to find a solution $u = u(t)$ having the given initial conditions:

$$\begin{aligned} u(0) &= d_0 \\ \dot{u}(0) &= v_0 \end{aligned} \tag{3}$$

where d_0 is the initial displacement and v_0 is the initial velocity. To start the process, the initial acceleration can be computed from $\ddot{u}(0) = [f(0) - c\dot{u}(0) - ku(0)]/m$.

The Newmark method (1959) can be used to solve the above initial value problem and has the following formulation:

$$\begin{aligned} ma_{n+1} + cv_{n+1} + kd_{n+1} &= f_{n+1} \\ d_{n+1} &= d_n + (\Delta t)v_n + (\Delta t)^2\left[\left(\frac{1}{2} - \beta\right)a_n + \beta a_{n+1}\right] \\ v_{n+1} &= v_n + (\Delta t)[(1-\gamma)a_n + \gamma a_{n+1}] \end{aligned} \tag{4}$$

where d_n, v_n and a_n are the approximations of displacement, velocity and acceleration, respectively. The subscript (n) indicates the time step at $t = n(\Delta t)$. The numerical characteristics of this method are controlled by the parameters β and γ. If $\beta = 0$ and $\gamma = 1/2$, this method reduces to the Newmark explicit method which is often used in pseudodynamic tests. The most commonly used constant average acceleration method for the nonlinear dynamic analysis also can be obtained by simply setting $\beta = 1/4$ and $\gamma = 1/2$.

If the equation of motion, i.e., Eq. (2), is integrated with respect to time once from t_0 to t, it becomes:

$$m\dot{u} + cu + k\overline{u} = \overline{f} \tag{5}$$

where $m\dot{u}(t_0) + cu(t_0) + k\overline{u}(t_0) = \overline{f}(t_0)$ is assumed, and $\overline{u}$ and $\overline{f}$ are introduced to represent the time integral of displacement and the time integral of external force, respectively. In order to be consistent with the use of $r = ku$, the symbol $\overline{r} = k\overline{u}$ is introduced to represent the time integral of restoring force for a nonlinear system. The initial value problem for Eq. (5) becomes to find a solution $\overline{u} = \overline{u}(t)$ having the same given initial conditions shown in Eq. (3). In this case, the initial value of the time integral of restoring force can be evaluated by $\overline{r}(0) = [\overline{f}(0) - m\dot{u}(0) - cu(0)]$. The initial value $\overline{f}(0)$ for an earthquake input can be taken to be zero since in the first few steps the amplitude of an ground acceleration record is almost zero while for an analytical expression of external force, it can be obtained mathematically. For example, if $f(t) = a\sin(\omega^* t)$ is assumed, one has $\overline{f}(t) = -(a/\omega^*)\cos(\omega^* t)$. Thus, $\overline{f}(0) = -(a/\omega^*)$ at $t = 0$. The Newmark integration method also can be applied to solve this integrated equation of motion with a slight modification and can be expressed as:

$$\begin{aligned} mv_{n+1} + cd_{n+1} + ks_{n+1} &= \overline{f}_{n+1} \\ s_{n+1} &= s_n + (\Delta t)d_n + (\Delta t)^2\left[\left(\frac{1}{2} - \beta\right)v_n + \beta v_{n+1}\right] \\ d_{n+1} &= d_n + (\Delta t)[(1-\gamma)v_n + \gamma v_{n+1}] \end{aligned} \tag{6}$$

where s_n is used to denote the approximation to $\overline{u}(t_n)$, the theoretical integral of the displacement at $t = t_n$. Unlike the currently available step-by-step integration methods, the time integral of external force is used to take place of the external force in this formulation.

It should be mentioned that the application of time integration technique to a step-by-step integration method is entirely different from the algorithms developed by O.C. Zienkiewicz where a finite element-weighted residual approach is applied in the detailed derivations (Zienkiewicz 1977 & 1977). In that approach, a specific shape function is employed to derive a specific direct integration method and there is no conversion of equation of motion from the second-order to the first-order. In addition, all the algorithms developed by O.C. Zienkiewicz are used to solve the equations of motions while the integrated equations of motion are solved by the proposed step-by-step integration method.

3. Implementation of the integral form of Newmark method

In order to demonstrate the practical applications of the integral form of Newmark method in the time history analysis, a possible implementation of the algorithm is sketched. The following detailed implementation of the algorithm is constructed for a single-degree-of-freedom system. However, it can be extended to a multi-degree-of-freedom system easily.

In Eq. (6), the second and third equations can be rewritten in terms of d_{n+1} and substituted into the first equation. Thus, the following equation, which will determine d_{n+1}, can be formulated after

some algebraic manipulations:

$$Wd_{n+1} = b \tag{7}$$

where

$$W = \frac{1}{\gamma(\Delta t)}m + c + \frac{\beta(\Delta t)}{\gamma}k \tag{8}$$

and

$$b = \overline{f}_{n+1} - ks_n + \left[\left(\frac{1}{\gamma}\right)\left(\frac{m}{\Delta t}\right) + \left(\frac{\beta-\gamma}{\gamma}\right)(\Delta t)k\right]d_n + \left[\left(\frac{1-\gamma}{\gamma}\right)m + \left(\frac{\beta-\frac{1}{2}\gamma}{\gamma}\right)(\Delta t)^2 k\right]v_n \tag{9}$$

Next, the velocity term v_{n+1} can be computed from the third equation of Eq. (6) and the time integral of displacement s_{n+1} can be obtained from the first equation of Eq. (6). This procedure is almost the same as that of the original form of the Newmark method for a linear system, except the changes of parameters from acceleration, velocity, displacement and external force to velocity, displacement, the time integral of displacement and the time integral of external force, respectively. Thus, there are no extra computational efforts required for this implementation except the time integral of external force. For a nonlinear system, Eq. (9) can rewritten as:

$$b = \overline{f}_{n+1} - \overline{r}_n + \frac{m}{\gamma(\Delta t)}d_n + \frac{\beta-\gamma}{\gamma}(\Delta t)r_n + \frac{1-\gamma}{\gamma}mv_n + \frac{\beta-\frac{1}{2}\gamma}{\gamma}(\Delta t)^2 kv_n \tag{10}$$

In this expression, the restoring force can be obtained from the computed displacement and then be integrated to yield the time integral of the restoring force. If the variation of the resistance within each time step is to be considered, more computational efforts are required in nonlinear dynamic analysis. This will be thoroughly discussed later.

4. The smoothing effect of time integration

The numerical characteristics of the constant average acceleration method and its integral form are evaluated in terms of solutions it generate for a simple pilot problem in which $f(t) = Z\sin(\omega^* t)$ in order to have an insight into the smoothing effect of time integration. The symbol Z is the amplitude and ω^* is the circular frequency of the harmonically varying load.

The numerical solutions obtained by using the integral form of the constant average acceleration method can be rewritten in a recursive matrix form (Bathe and Wilson 1973, Bathe 1982, Belytschko and Hughes 1983, Hilber *et al.* 1977, Hughes 1987, Zienkiewicz 1977):

$$\overline{\boldsymbol{X}}_{\boldsymbol{n+1}} = \boldsymbol{A}\overline{\boldsymbol{X}}_{\boldsymbol{n}} + \boldsymbol{L}\overline{f}_{n+1} = \boldsymbol{A}^{(n+1)}\overline{\boldsymbol{X}}_0 + \sum_{i=0}^{n}\boldsymbol{A}^{(n-i)}\boldsymbol{L}\overline{f}_{i+1} \tag{11}$$

where $\overline{\boldsymbol{X}}_{\boldsymbol{n}}$ is defined as:

$$\overline{\boldsymbol{X}}_{\boldsymbol{n}} = \begin{bmatrix} s_n \\ (\Delta t) d_n \\ (\Delta t)^2 v_n \end{bmatrix} \tag{12}$$

and $\overline{f}_i$ is the time integral of the given sinusoidal force and it is:

$$\overline{f}_i = -\frac{Z}{\omega^*}\cos(\omega^* t_i) \tag{13}$$

The amplification matrix $\boldsymbol{A}$ and the load factor $\boldsymbol{L}$ are found to be:

$$\boldsymbol{A} = \frac{1}{4+\Omega^2}\begin{bmatrix} 4 & 4 & 1 \\ -2\Omega^2 & 4-\Omega^2 & 2 \\ -4\Omega^2 & -4\Omega^2 & -\Omega^2 \end{bmatrix} \tag{14}$$

and

$$\boldsymbol{L} = \frac{\Omega^2}{k(4+\Omega^2)}\begin{bmatrix} 1 \\ 2 \\ 4 \end{bmatrix} \tag{15}$$

in which $\Omega = \omega(\Delta t)$ and ω is the natural frequency of the single-degree-of-freedom system. It is worth noting that at the beginning of motion the integral of external force is not equal to zero and is found to be $\overline{f}_0 = -Z/\omega^*$ which is derived from Eq. (13) at $t = t_0 = 0$. Thus, for the case of $d_0 = 0$ and $v_0 = 0$, the initial value of the time integral of displacement is found to be:

$$s_0 = \frac{1}{k}(\overline{f}_0 - m v_0 - c d_0) = -\frac{Z}{k\omega^*} \tag{16}$$

This implies $\overline{\boldsymbol{X}}_0 = [-Z/(k\omega^*),\ 0,\ 0]^T$.

To evaluate the characteristics for capturing the harmonically varying load, it is desirable to obtain from Eq. (11) a closed-form expression for the displacement. By means of spectral decomposition (Strang 1986) of the matrix $\boldsymbol{A}$, one can obtain from Eq. (11) that

$$\begin{aligned}(\Delta t) d_{n+1} = {} & [a\cos(n\overline{\Omega}) + b\sin(n\overline{\Omega})] + \frac{2\Omega^2}{k(4+\Omega^2)}\,\overline{f}_{n+1} \\ & + \sum_{i=0}^{n-1}\{c\cos[(n-i-1)\overline{\Omega}] + d\sin[(n-i-1)\overline{\Omega}]\}\,\overline{f}_{i+1}\end{aligned} \tag{17}$$

where $\overline{\Omega} = \overline{\omega}(\Delta t)$ and the apparent numerical frequency $\overline{\omega}$ is given by the following equation:

$$\overline{\omega} = \frac{1}{\Delta t}\tan^{-1}\left(\frac{4\Omega}{4-\Omega^2}\right) \tag{18}$$

The coefficients *a*, *b*, *c* and *d*, which are determined from Eq. (11) by matching the initial conditions, can be expressed as:

$$a = \left(\frac{Z}{k}\right)\frac{2\Omega^2}{\Omega^*(4+\Omega^2)}$$

$$b = \left(\frac{Z}{k}\right)\frac{4\Omega}{\Omega^*(4+\Omega^2)}$$

$$c = \left(\frac{1}{k}\right)\frac{4\Omega^2(4-\Omega^2)}{(4+\Omega^2)^2}$$

$$d = \left(\frac{1}{k}\right)\frac{-16\Omega^3}{(4+\Omega^2)^2} \tag{19}$$

After substituting Eq. (19) into Eq. (17) and some algebraic manipulations, Eq. (17) becomes:

$$d_{n+1} = \left(\frac{Z}{k}\right)\{A^i_{ave}\sin[(n+1)\Omega^*] - B^i_{ave}\sin[(n+1)\overline{\Omega}]\} \tag{20}$$

where

$$A^i_{ave} = \frac{\Omega\sin(\overline{\Omega})\sin(\Omega^*)}{2\Omega^*[\cos(\Omega^*)-\cos(\overline{\Omega})]}$$

$$B^i_{ave} = \frac{\Omega[1+\cos(\overline{\Omega})][1-\cos(\Omega^*)]}{2\Omega^*[\cos(\Omega^*)-\cos(\overline{\Omega})]} \tag{21}$$

in which the subscript (*ave*) and the superscript (*i*) combine to stand for the use of the integral form of the constant average acceleration method to yield the discrete solutions.

The closed-form expression for the displacement using the constant average acceleration method also can be derived by the same procedure. As a result, the recursive numerical solutions obtained by using this integration method are:

$$\boldsymbol{X_{n+1}} = \boldsymbol{A}\boldsymbol{X_n} + \boldsymbol{L}f_{n+1} = \boldsymbol{A}^{(n+1)}\boldsymbol{X_0} + \sum_{i=0}^{n}\boldsymbol{A}^{(n-i)}\boldsymbol{L}f_{i+1} \tag{22}$$

where $\boldsymbol{X_n}$ and f_i are:

$$\boldsymbol{X_n} = \begin{bmatrix} d_n \\ (\Delta t)v_n \\ (\Delta t)^2 a_n \end{bmatrix} \tag{23}$$

and

$$f_i = Z\sin(\omega^* t_i) \tag{24}$$

For the case of free vibration, one has $\boldsymbol{X}_0 = [0, 0, 0]^T$. Finally, for this free vibration case, the closed-form expression for the displacement can be derived from Eq. (22) and is:

$$d_{n+1} = \left(\frac{Z}{k}\right)\{A_{ave}\sin[(n+1)\Omega^*] - B_{ave}\sin[(n+1)\bar{\Omega}]\} \tag{25}$$

where

$$A_{ave} = \frac{\sin(\bar{\Omega})\left\{\sin(\bar{\Omega}) + \tan\left(\frac{1}{2}\bar{\Omega}\right)[\cos(\Omega^*) - \cos(\bar{\Omega})]\right\}}{2[\cos(\Omega^*) - \cos(\bar{\Omega})]}$$

$$B_{ave} = \frac{\sin(\bar{\Omega})\sin(\Omega^*)}{2[\cos(\Omega^*) - \cos(\bar{\Omega})]} \tag{26}$$

in which the subscript (*ave*) indicates that the discrete solutions are obtained from the constant average acceleration method.

The exact solution of the single-degree-of-freedom system subjected to the harmonically varying load of $f(t) = Z\sin(\omega^* t)$ can be obtained by the analytical method (Clough and Penzien 1967) and is equal to:

$$d(t) = \left(\frac{Z}{k}\right)[A_{exa}\sin(\omega^* t) - B_{exa}\sin(\omega t)] \tag{27}$$

where

$$A_{exa} = \frac{\Omega^2}{\Omega^2 - (\Omega^*)^2}$$

$$B_{exa} = \frac{\Omega\Omega^*}{\Omega^2 - (\Omega^*)^2} \tag{28}$$

The subscript (*exa*) represents that the analytical method is used to solve the equation of motion. Since the solution is composed of the steady-state component and the transient component of the response, the weight of each component will play an important role in the total effect. Therefore, it is very important to estimate each contribution to the total response. For this purpose, the contribution coefficients C_S and C_T which correspond to the steady-state response and the transient response, respectively, are defined as follows:

$$C_S = \frac{|A_{exa}|}{|A_{exa}| + |B_{exa}|}$$

$$C_T = \frac{|B_{exa}|}{|A_{exa}| + |B_{exa}|} \tag{29}$$

It should be mentioned that the contribution coefficients C_S and C_T generally do not represent the realistic contributions for the transient and the steady-state responses, respectively, since only the

absolute amplitudes are considered. However, they still can provide a very valuable information for the two response components of the total effect. If we define the response contribution ratio R as C_T over C_S, the following relationship can be found:

$$R = \frac{C_T}{C_S} = \frac{T}{T^*} \tag{30}$$

This indicates that the response contribution ratio R is equal to the ratio of the natural vibration period of the system T to the applied natural period of the given harmonic loading T^*. In this expression, it is likely to be true that the transient response is greater than the steady-state response if the natural vibration period is larger than the natural applied driving period and vice versa.

In order to evaluate the capability to capture the rapid changes of dynamic loading possessed by the constant average acceleration method and its integral form, four relative amplitude errors are defined as follows.

$$\begin{aligned} S_{ave} &= \left|\frac{A_{ave}}{A_{exa}} - 1\right|, \quad T_{ave} = \left|\frac{B_{ave}}{B_{exa}} - 1\right| \\ S^i_{ave} &= \left|\frac{A^i_{ave}}{A_{exa}} - 1\right|, \quad T^i_{ave} = \left|\frac{B^i_{ave}}{B_{exa}} - 1\right| \end{aligned} \tag{31}$$

The symbols T and S are introduced to stand for the relative amplitude errors for the transient response and the steady-state response, respectively. The superscript i indicates the integral form of the integration method. For example, S^i_{ave} is the relative amplitude error for the steady-state response if using the integral form of the constant average acceleration method. By substituting Eqs. (21), (26) and (28) into Eq. (31), it can be found that T_{ave} is exactly equal to S^i_{ave}. All the four relative amplitude errors defined above are plotted in Figs. 1 to 6 for the values of R = 1/4, 1/2, 3/4, 2.5, 5, and 10. Figs. 1 to 3 are in the case of $R < 1$ and Figs. 4 to 6 are in the case of $R > 1$. For all the figures, the top x-axis represents the value of $\Delta t/T$ and the bottom x-axis is used to represent the value of $\Delta t/T^*$. It will be automatically assumed that only the interval of $\Delta t/T \le 0.056$ is considered in the following discussions since in this interval the constant average acceleration method and its integral form can provide an accurate solution with a relative period error less than 1%.

It can be found from Figs. 1 to 3 that all the four relative amplitude errors for a given value of $\Delta t/T$ increase with the value of R from 0 to 1. This clearly indicates that, for both integration methods, the capability to capture the rapid changes of sinusoidal force is decreased as the value of R increases from 0 to 1. All the three figures also show that, for a given value of $\Delta t/T$, the relative amplitude errors of the integral form of the constant average acceleration method are larger than that of the constant average acceleration method both in the steady-state response and in the transient response. This means that for a same time step the constant average acceleration method provides more accurate results than that of its integral form for $R < 1$. However, for a same time step, the integral form of the constant average acceleration method still can give comparable results as that obtained from the constant average acceleration method. This can be explained by two considerations. First, for a small R (say $R < 1/2$), all the relative amplitude errors are very small for both direct integration methods. Secondly, the difference of the relative amplitude errors in the

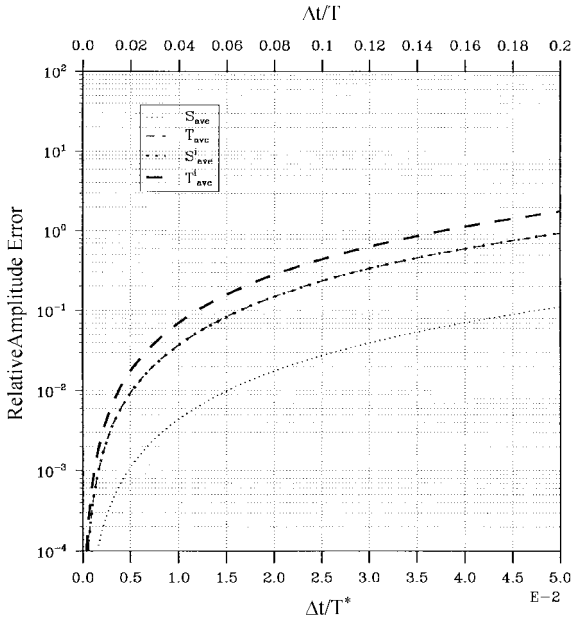

Fig. 1 Variation of relative amplitude error for $R = 1/4$

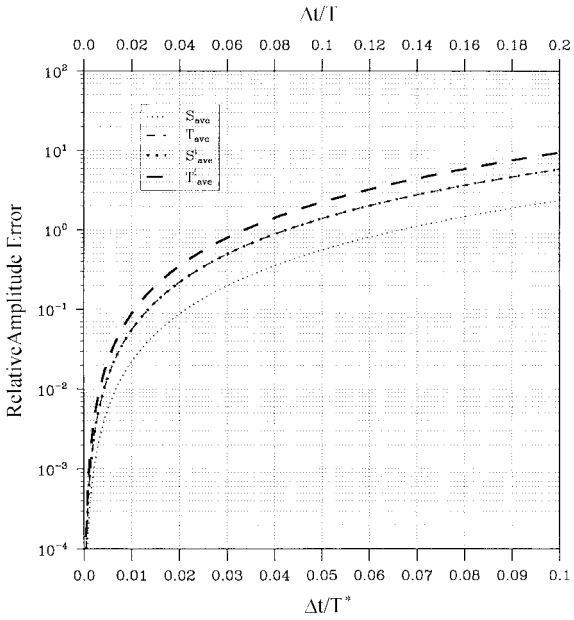

Fig. 2 Variation of relative amplitude error for $R = 1/2$

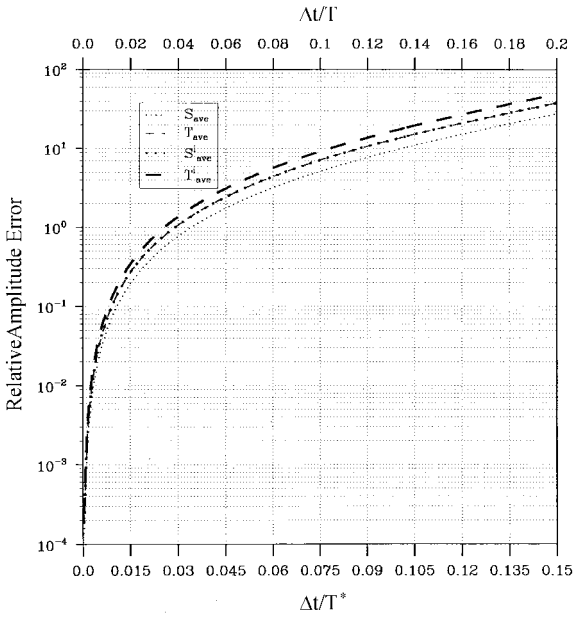

Fig. 3 Variation of relative amplitude error for $R = 3/4$

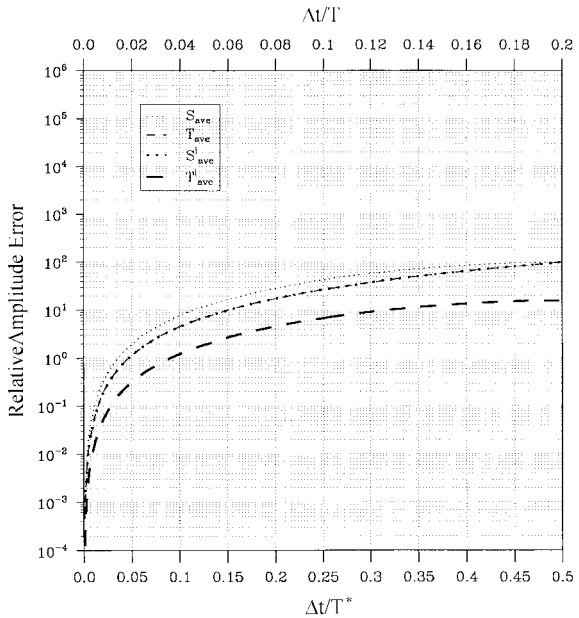

Fig. 4 Variation of relative amplitude error for $R = 2.5$

transient or the steady-state response between the two integration methods becomes smaller and smaller as R increases from 0 to 1. It also can be seen that for $R < 1$ the relative amplitude error for

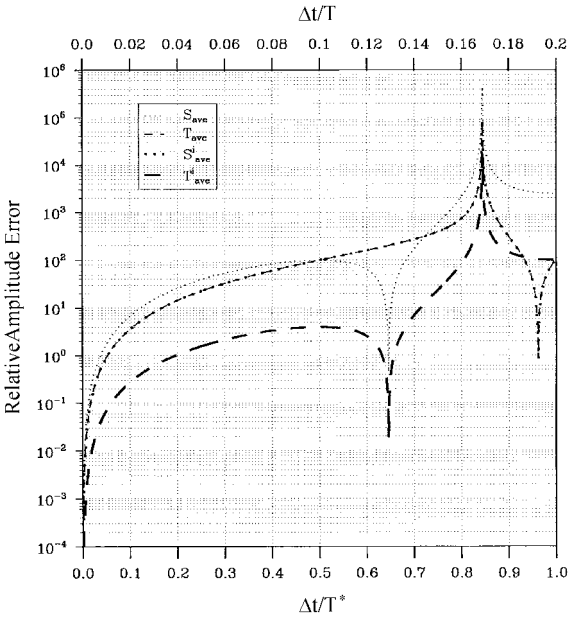

Fig. 5 Variation of relative amplitude error for $R = 5$

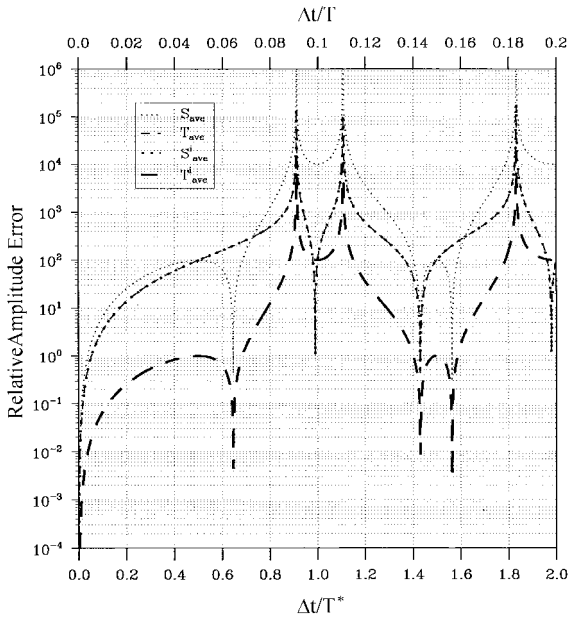

Fig. 6 Variation of relative amplitude error for $R = 10$

the transient response is greater than for the steady-state response for both integration methods.

On the contrary to the case of $R < 1$, the relative amplitude errors of the integral form of the constant average acceleration method are less than that of the constant average acceleration method both in the steady-state and in the transient responses for $R > 1$ as shown in Figs. 4 to 6. This is the key factor to give the integral form of the constant average acceleration method a better capability to capture the rapid changes of harmonic loading than that of the constant average acceleration method. In addition, this effect becomes more significant as the value of R becomes larger. This is because that the curves for S_{ave}, T_{ave} and S^i_{ave} move upward with the increase of R while the curve of T^i_{ave} is almost invariant with R for $\Delta t/T<0.056$. It should be mentioned here that "the larger the value of R, the more contribution from the transient response" is also an important factor to explain this effect. In the case of $R > 1$, for a given value of $\Delta t/T$, the relative amplitude error for the transient response less than that for the steady-state response for both integration methods is also observed.

It has been found that for both integration methods if $C_S > C_T$ ($R < 1$) than $T_{ave} > S_{ave}$ ($T^i_{ave} > S^i_{ave}$) and if $C_S < C_T$ ($R > 1$) than $T_{ave} < S_{ave}$ ($T^i_{ave} < S^i_{ave}$). Obviously, this effect is in favor of both integration methods for accurate integration of the structural response since a large relative amplitude error always corresponds to a small contribution coefficient and a small relative amplitude error is always correspondent to a large contribution coefficient for any value of R.

As a summary of this study, the constant average acceleration method and its integral form have about the same capability in capturing the variation of harmonic loading for $R < 1$. However, for $R > 1$ this capability possessed by the integral form of the constant average acceleration method is better than that of the constant average acceleration method, especially for a large value of R.

5. The upper bounds of $\Delta t/T$ for accurate integration of linear systems

In order to investigate the advantages of using the integral form of the constant average acceleration method in performing the step-by-step dynamic analysis, the upper bound of $\Delta t/T$ as a function of R for linear systems is explored for both integration methods, using a specific required accuracy. We would like to establish this upper bound for $\Delta t/T$ so that the period distortion is not greater than 1% and the amplitude growth or decay is less than 3% after ten times of the period of a single-degree-of-freedom system.

For this purpose, the response of a single-degree-of-freedom system subjected to a harmonically varying load is computed by using the constant average acceleration method and its integral form. The natural period of the system is designed to be 1 sec. The motion starts from the rest and the sinusoidal force is given as:

$$f(t) = 500 \sin\left(\frac{2\pi}{T^*} t\right) \tag{32}$$

The results for the upper bound of $\Delta t/T$ for accurate integration of a linear single-degree-of-freedom system subjected to a sinusoidal force are depicted in Fig. 7 where least-squares fit with fixed knots is used to produce the two curves. Obviously, for both integration methods, the capability to trace the rapid changes of dynamic loading highly depends upon the value of R. It is clear that these two curves drop very sharply from $R = 0$ to $R = 1$, then increase less steeply until $R = 2$ for the constant average acceleration method and $R = 4$ for the integral form, finally they both decrease gradually. It is worth noting that there is a big spike as R closes to 1 for both integration methods. This might be due to the resonant effect.

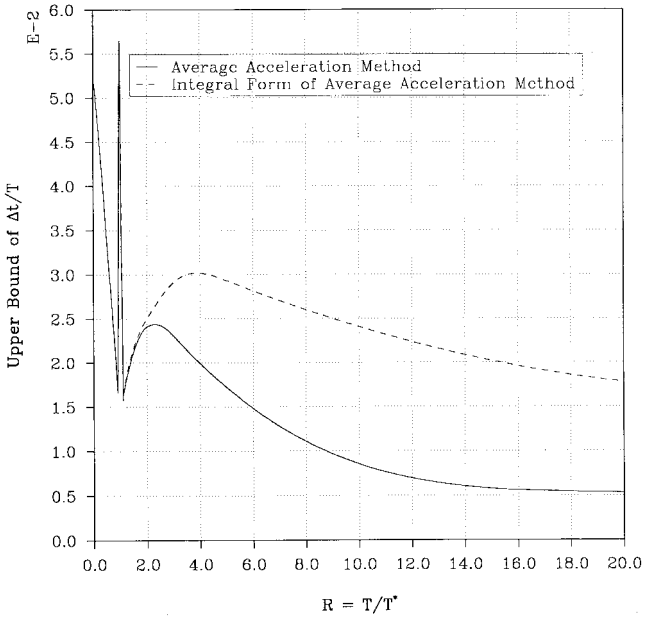

Fig. 7 Upper bound of $\Delta t/T$ versus T/T^*

In general, for accurate integration of linear systems, both integration methods have roughly the same upper bounds of $\Delta t/T$ in the range of $R < 2$. On the other hand, for $R > 2$ the integral form of the constant average acceleration method has larger upper bounds than that of the constant average acceleration method and this phenomenon seems to become more significant with the increase of R. This clearly indicates that using a same time step the integral form of the constant average acceleration method possesses better capability to trace the rapid changes of harmonic loading than that of the constant average acceleration method as $R > 2$ while for $R < 2$ both integration methods can provide almost the same accurate solutions. These upper bounds obtained here are in good agreement with the theoretical study results in the above section.

This figure also shows that to yield reliable solutions based on this criterion, the size of time step is almost controlled by the capability to trace the rapid changes of dynamic loading and not by the linear accuracy consideration. This is because that almost all the upper bounds of $\Delta t/T$ for accurate integration of linear systems subjected to a harmonic load are less than 0.056. For the case of $\Delta t/T = 0.056$, the constant average acceleration method and its integral form will introduce 1% of the relative period distortion error that is the maximum value of the criterion to construct these upper bounds. It should be mentioned that for nonlinear systems the presence of nonlinearity is also a very stringent constraint in the size of time step. In fact, in general, for a highly nonlinear system, it might use a time step much smaller than that required by the accuracy consideration or the capability to capture the rapid changes of dynamic loading to reduce or eliminate the linearization error (Chang 1994).

6. Numerical examples

In the following investigations, some linear examples are proposed to illustrate the advantages of using the integral form of the constant average acceleration method in tracing the rapid changes of dynamic loading. It should be mentioned that the use of linear systems is intended to avoid dealing with the difficulties caused by the abrupt changes in stiffness due to yielding or unloading or the smooth variation of resistance due to material and/or geometric nonlinearities. The loading cases for a harmonically varying load, an earthquake load and an impact load are considered.

6.1 Example(1). A harmonic input

The single-degree-of-freedom system and the sinusoidal force used previously in the development of the upper bounds of $\Delta t/T$ are also employed here. The applied natural period T^* is set to be 0.1 sec and, thus, $R = 10$ for $T = 1$ sec. The forced vibration responses obtained by using both integration methods are shown in Fig. 8. The numerical results are considered as the "***exact***" solutions if using the constant average acceleration method with a time step of 0.005 sec. The integral form of the constant average acceleration method provides very accurate results by using a time step of 0.025 sec while for this time step the solutions obtained from the constant average acceleration method are deviated significantly from the exact solutions. This can be explained by Fig. 7. It indicates that to obtain reliable results for $R = 10$ by using the constant average acceleration method, the size of time step must be less than 0.008 sec. In other words, in this case the constant average acceleration method requires a time step about one-third of that used by the integral form of the constant average acceleration method to yield an accurate result.

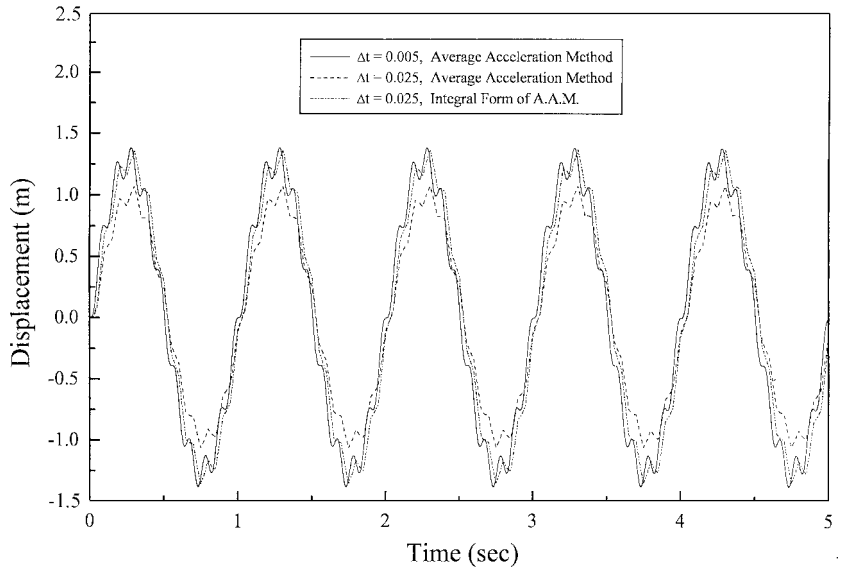

Fig. 8 Response of a SDOF system for T = 1.0 and T^* = 0.1

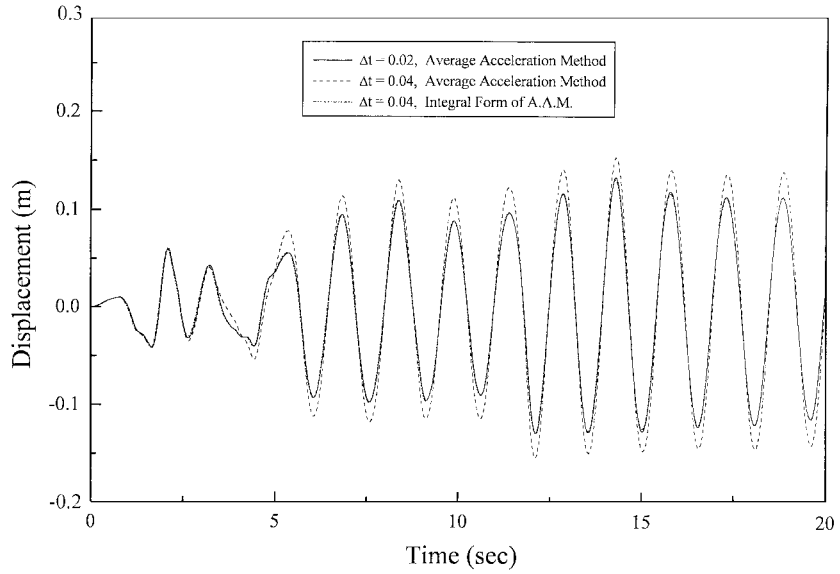

Fig. 9 Response of a SDOF system subjected to El Centro EQ

6.2 Example(2). An earthquake input

In this example, a single-degree-of-freedom system whose period is 1.5 sec is considered. The system is subjected to the 1940 El Centro earthquake record by scaling its peak ground acceleration to 0.25 g. This corrected accelerogram has been presented as values given every 0.02 sec. The time

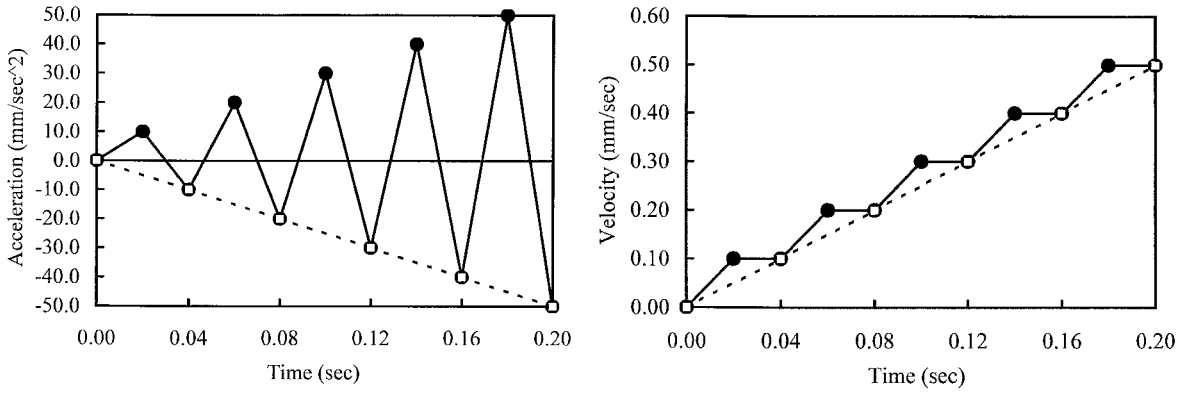

Fig. 10 Effect of time integration for digital data

history response of this system is shown in Fig. 9. The solutions obtained from the constant average acceleration method using a time step of 0.02 sec are considered as *"**exact**"* solutions. Both integration methods are also employed to perform the dynamic analysis with a time step of 0.04 sec. The sub-step size of 0.02 sec is used to obtain the time integral of external force for the application of the integral form method. Again, the integral form of the constant average acceleration method gives very accurate solutions while a very significant amplitude growth is observed by using the constant average acceleration method. This is due to the fact that the digital data with a high-frequency content has been smoothed out and an extra data point within the time step was taken into account by the procedure of time integration for using the integral form of the constant average acceleration method.

Fig. 10 is used to schematically illustrate the effect of the time integration of a set of digital data. All the data points connected by solid lines have the equal time interval of 0.02 sec and those connected by dotted line are 0.04 sec. The upper plot shows the assumed ground acceleration data points and the corresponding ground velocity data points are shown in the lower plot. The velocity data are obtained from integrating the acceleration data with time once using the trapezoidal rule with a time increment of 0.02 sec. It is clear that the changes of the acceleration data or velocity data can be entirely captured if the step size of 0.02 sec is used to perform the time integration. On the other hand, if the time step of 0.04 sec is used, the characteristics of the acceleration data as indicated by the dotted line in the upper plot are totally misleading. Meanwhile the characteristics of the velocity data as shown by the dotted line in the lower plot still can be simulated very reliably. Obviously, this is because that the middle data point is not considered for the acceleration while it is taken into account for the velocity through the time integration.

6.3 Example(3). An impact problem

The impact problem for a one-dimensional uniform steel bar with one end fixed and the other end free is considered. The bar is initially at rest and the tip loading is imposed at the free end. Fig. 11 shows the bar and the shape of the half-sine impulse whose maximum amplitude is $P_0 = 1000$ N and the loading duration is $t_d = 1.0 \times 10^{-7}$ sec. The structural properties of the steel bar are: $A = 625$ mm^2, $E = 2.0 \times 10^5$ N/mm^2, $\rho = 8.0 \times 10^{-9}$ N-sec^2/mm^4 and $L = 500$ mm.

The steel bar is modeled by using 40 truss elements and its highest frequency is found to be

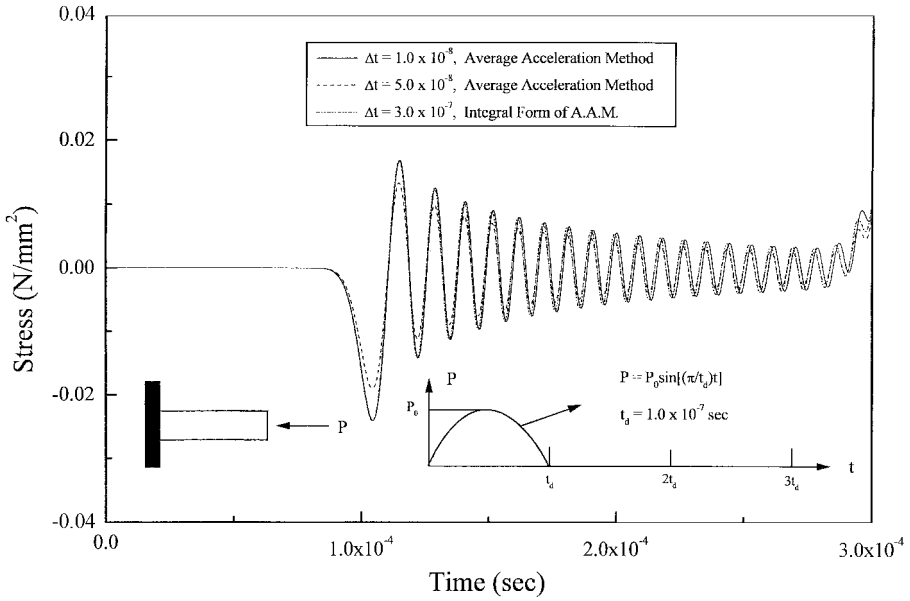

Fig. 11 Stress time history at the fixed end for the steel bar

8.0×10^5 rad/sec. Unlike the structural dynamic problems where only the low frequency modes are of interest, all the modes must be integrated accurately to obtain reliable results for the impact problem since for an impact problem the response contributions from the high frequency modes are also very important (Belytschko and Hughes 1983, Clough and Penzien 1967). Both the constant average acceleration method and its integral form are used to solve the impact problem. In Fig. 11, the results obtained from the constant average acceleration method with the step size of 1.0×10^{-8} sec are considered as "***exact***" solutions. The constant average acceleration method with the use of a time step of 5.0×10^{-8} sec cannot provide accurate results while the integral form of the constant average acceleration method using $\Delta t = 3.0 \times 10^{-7}$ sec still gives acceptable solutions. This is because that the time integral of external force can effectively capture the characteristics of the external force even though the step size is 3 times of the duration of the short impulse. It is worth noting that it is impossible for any currently available integration methods to use a step size bigger than the duration of an impulse to yield accurate results. The CPU time for each case is listed below:

Case	Integration method	Time step	CPU
1	Ave. Acc. method	$\Delta t = 1.0 \times 10^{-8}$	129.25 sec
2	Ave. Acc. method	$\Delta t = 5.0 \times 10^{-8}$	26.29 sec
3	Integral form of A.A.M.	$\Delta t = 3.0 \times 10^{-7}$	4.17 sec

It is clear from this table that the saving of computational efforts for the integral form of constant average acceleration method is very significant.

The improved capability in capturing the rapid changes of dynamic loading for the integral form of the constant average acceleration method is manifested by the three numerical examples. The

favorable smoothing effect of time integration eliminates the need of using a very small time step to capture the rapid changes of dynamic loading.

7. Linearization errors

In the step-by-step integration, the errors introduced by the assumption that the structural properties remain constant during each time step will be termed "***linearization errors***". These errors will be carried to subsequent computations. Consequently, the numerical result in any step depends upon an interaction from every previous step. Owing to this cumulative error propagation effect and the large number of steps, numerical results may diverge significantly from the correct solutions, even though errors introduced in a single step are relatively small. In a linear system, there will be no linearization error since the actual structural properties of the system are actually constant in a time step, which is consistent with the basic assumption of linearized approximations. On the other hand, for a nonlinear system the linearization errors may be caused by the rapid changes in stiffness due to yielding or unloading or the smooth variation of resistance due to material and/or geometric nonlinearities.

In the currently available direct integration methods, this linearization problem is, in general, overcome by using a very small time step or by using an iterative procedure where the structural properties are updated in the time interval to reduce or eliminate the linearization errors (Chang 1994). It seems that the time integration technique can provide a new way to deal with the linearization problem since the variation of restoring force within each time step can be taken into account appropriately through the time integration of the restoring force. Fig. 12 schematically explores the advantage of using the time integration technique. In this figure, the big arc area is the linearization error occurred in the $(n + 1)$-th time step if the variation of the restoring force within the step is not taken into account. On the other hand, if the original time step is subdivided into 3 equal sub-steps, the linearization error will be significantly reduced to the sum of the three small arc

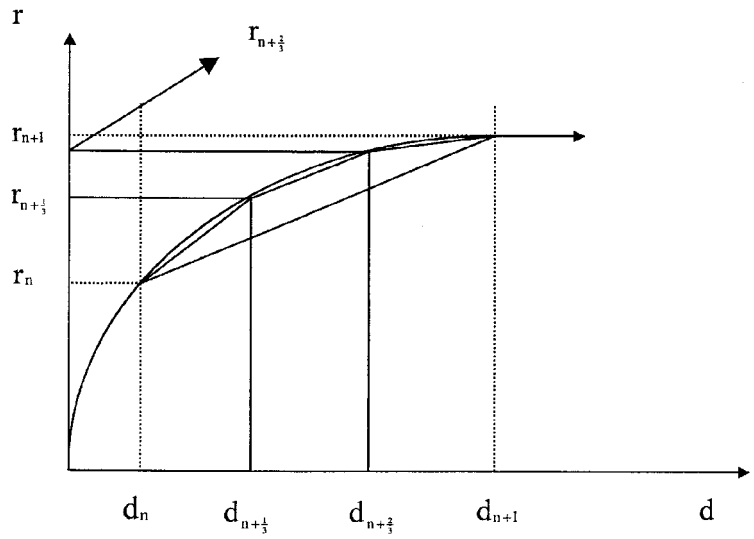

Fig. 12 The smooth variation of the restoring force

areas. This is because that the restoring forces, $r_{n+1/3}$ and $r_{n+2/3}$, are considered in the computations of the time integration of the restoring forces.

In order to illustrate that the time integral of the restoring force can effectively reduce linearization errors, we consider an undamped single-degree-of-freedom system whose mass is 1 kg and stiffness is taken as a function of displacement u with the unit of N/m. In fact, the stiffness is

$$k = 4\pi^2(1 + \alpha u^p) \tag{33}$$

where $4\pi^2$ is the initial stiffness, α is the coefficient of the nonlinear structural stiffness and p is an integer exponent that describes the nature of the nonlinearity. If p is even, the system possesses a hardening characteristic for positive α and a softening characteristic for negative α. The external force is given as $f(t) = 50\cos(10t)$N.

The displacement responses for a hardening system with $p = 2$ and $\alpha = 0.1$ and a softening system with $p = 2$ and $\alpha = -0.05$ are plotted in Figs. 13 and 14, respectively. In this example, two different cases as indicated in Fig. 12 are considered for the computation of the integration of the restoring force when the integral form of the constant average acceleration method is employed. The following equations are obtained from the direct applications of the trapezoidal rule and will be used to compute the time integral of restoring force $\overline{r}_{n+1}$.

$$\text{Scheme (a)} \qquad \overline{r}_{n+1} = \overline{r}_n + \frac{1}{2}(\Delta t)(r_n + r_{n+1})$$

$$\text{Scheme (b)} \qquad \overline{r}_{n+1} = \overline{r}_n + \frac{1}{2}(\Delta t)\left(r_n + 2r_{n+\frac{1}{3}} + 2r_{n+\frac{2}{3}} + r_{n+1}\right) \tag{34}$$

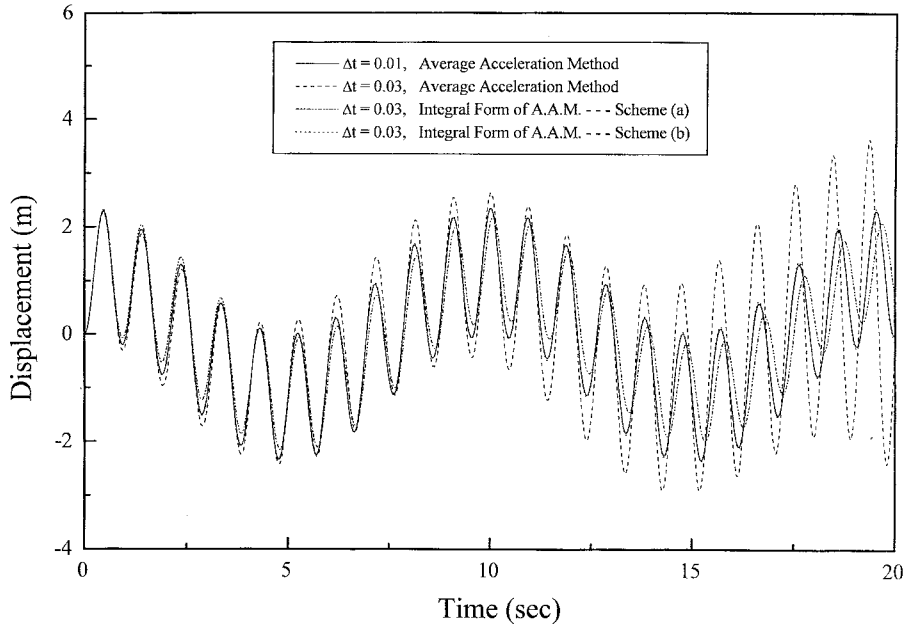

Fig. 13 Response of a hardening system for $f(t) = 50\cos(10t)$

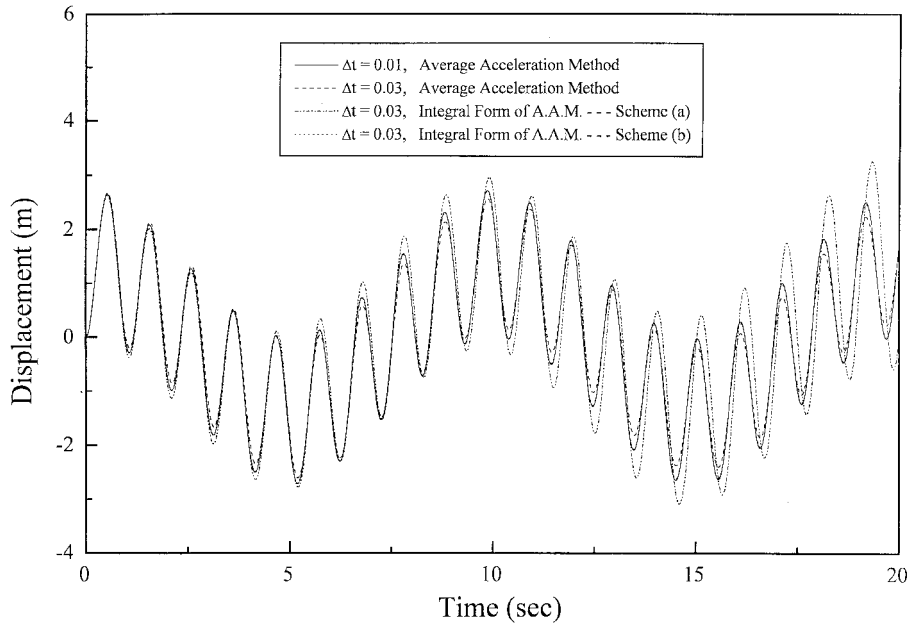

Fig. 14 Response of a softening system for $f(t) = 50\cos(10t)$

where the terms $r_{n+1/3}$ and $r_{n+2/3}$ each represents the restoring force at $t = t_n + \frac{1}{3}(\Delta t)$ and $t = t_n + \frac{2}{3}(\Delta t)$, respectively. Scheme (a) implies that only the restoring forces at the beginning and the end of the step are taken into account while for the use of Scheme (b) two extra values of the restoring forces are used to compute $\overline{r}_{n+1}$. In Figs. 13 and 14, numerical solutions obtained from the constant average acceleration method with a time step of 0.001 sec are considered as *"**exact**"* solutions. The results obtained from the constant average acceleration method and its integral form using Scheme (a) lead to unreliable results for both the hardening and softening system. Meanwhile the integral form of the constant average acceleration method with Scheme (b) gives very accurate results for both hardening and softening nonlinear systems. This indicates that the time integral of the restoring force can effectively reduced the linearization errors. This is also very promising in performing a pseudodynamic test since the restoring forces can be experimentally measured several times or even continuously within each time step and then be integrated to obtain the time integral of the restoring forces. The detailed explanations are in the next section.

7. Applications to pseudodynamic testing

The pseudodynamic method (Shing and Mahin 1984) is to solve the governing equations of motion by using a step-by-step integration method with experimental testing. This method is very similar to the conventional time history analysis using a direct integration method. A test specimen is first idealized as a discrete system such that the equations of motion for the system can be formulated. The inertial and viscous damping properties of the test structure are analytically formulated such that the dynamic characteristics of the system can be accurately represented. During a pseudodynamic test, the equations of motion are solved by means of a step-by-step

integration procedure. The displacements computed in each time step are imposed upon the test structure quasi-statically through servo-hydraulic actuators. The restoring forces developed by structural deformations are then measured by using load transducers, and are fed back to the next step displacement computations (Shing and Mahin 1984 & 1987 & 1990). This clearly indicates that the use of mathematical models of structural components to mimic the force-deformation relationships of the test structure is not required. In this procedure, an on-line digital computer is employed for all the numerical computations and experimental control.

Unlike the nonlinear dynamic analysis, no computation of the restoring force is needed in pseudodynamic tests since the restoring force within each time step can be experimentally measured many times or even continuously through a data acquisition system and be integrated to yield the time integral of the restoring force. Therefore, the variation of the resistance within each time step is totally considered and the linearization errors can be significantly reduced or eliminated. This advantage and the smoothing effect will make the time integration technique be very promising to improve the accuracy of a pseudodynamic test. In fact, it has been very successfully implemented in an actual test (Chang *et al.* 1998, Chang 1996).

8. Conclusions

In performing the step-by-step time history analysis, the superiority of solving the integrated equations of motion over the very commonly used equations of motion is further investigated in this paper. The capability to capture the harmonic loading for the use of the constant average acceleration method and its integral form is analytically evaluated and compared. Analytical results indicate that this capability for the integral form of the constant average acceleration method is much better than that of its original form. In addition, both are closely related to the ratio of the natural vibration period to the applied driving period. Thus, the smoothing effect of time integration is analytically confirmed since any dynamic loading can be considered as a combination of a series of harmonic loadings. It is also illustrated that it is possible to use a time step that is larger than the loading duration of an impulse in the solution of an impact problem or a wave propagation problem if the time integration technique is applied. This implies that the time integration technique is also very competitive in the time history analysis of impact problems or wave propagation problems.

Acknowledgements

The author is grateful to acknowledge that this study is financially supported by the National Science Council, Taiwan, R.O.C., under Grant No. NSC-90-2711-3-319-200.

References

Bathe, K.J. and Wilson, E.L. (1973). “Stability and accuracy analysis of direct integration methods”, *Earthq. Eng. and Struct. Dyn.*, **1**, 283-291.

Bathe, K.J. (1982). *Finite Element Procedures in Engineering Analysis*, Prentice-Hall, Inc., Englewood Cliffs, New Jersey.

Belytschko, T. and Hughes, T.J.R. (1983). *Computational Methods for Transient Analysis*, Elsevier Science Publishers B.V., North-Holland.

Chang, S.Y. (1994). "Improved dynamic analysis for linear and nonlinear systems", Ph.D. Thesis, Department of Civil Engineering, University of Illinois, Urbana-Champaign.

Chang, S.Y. (1996). "A series of energy conserving algorithms for structural dynamics", *J. Chinese Inst. Eng.*, **19**(2).

Chang, S.Y., Tsai, K.C. and Chen, K.C. (1998). "Improved time integration for pseudo-dynamic tests", *Earthq. Eng. and Struct. Dyn.*, **27**, 711-730.

Chang, S.Y. (1996). "The smoothing effect in structural dynamics and pseudodynamic tests", NCREE Report, NCREE-96-008, National Center for Research on Earthquake Engineering. Taipei, Taiwan, Republic of China.

Chen, C.C. and Robinson, A.R. (1993). "Improved time history analysis for structural dynamics. I: Treatment of rapid variation of excitation and material nonlinearity", *J. Eng. Mech.*, **119**(12), 2496-2513.

Clough, R.W. and Penzien, J. (1967). *Dynamics of Structures*, McGraw-Hill, New York.

Hilber, H.M., Hughes, T.J.R. and Taylor, R.L. (1977). "Improved numerical dissipation for time integration algorithms in structural dynamics", *Earthq. Eng. and Struct. Dyn.*, **5**, 283-292.

Houbolt, J.C. (1950). "A recurrence matrix solution for the dynamic response of elastic aircraft", *J. Aeronautical Sci.*, **17**, 540-550.

Hughes, T.J.R. (1987). *The Finite Element Method*, Prentice-Hall, Inc., Englewood Cliffs, N.J.

Newmark, N.M. (1959). "A method of computation for structural dynamics", *J. Eng. Mech. Div.*, ASCE, **85**, 67-94.

Park, K.C. (1975). "An improved stiffly stable method for direct integration of nonlinear structural dynamic equations", *J. Appl. Mech.*, **42**, 464-470.

Shing, P.B. and Mahin, S.A. (1984). "Pseudodynamic method for seismic performance testing: theory and implementation", UCB/EERC-84/01, Earthquake Engineering Research Center, University of California, Berkeley, CA.

Shing, P.B. and Mahin, S.A. (1987). "Cumulative experimental errors in pseudo-dynamic tests", *Earthq. Eng. and Struct. Dyn.*, **15**, 409-424.

Shing, P.B. and Mahin, S.A. (1990). "Experimental error effects in pseudodynamic testing", *J. Eng. Mech.*, ASCE, **116**, 805-821.

Strang, G. (1986). *Linear Algebra and Its Applications*, Harcourt Brace Jovanovich, San Diego.

Zienkiewicz, O.C. (1977). *The Finite Element Methods*, McGraw-Hill Book Company, UK.

Zienkiewicz, O.C. (1977). "A new look at the Newmark, Houbolt and other time stepping formulas. A weighted residual approach", *Earthq. Eng. and Struct. Dyn.*, **5**, 413-418.